Available online at www.sciencedirect.com
SCIENCE DIRECT
Polymer 46 (2005) 1125–1138
polymer
www.elsevier.com/locate/polymer

A round robin study for the characterization of latex particle morphology—multiple analytical techniques to probe specific structural features

Jeffrey M. Stubbs, Donald C. Sundberg*

Nanostuctured Polymers Research Center, Materials Science Program, University of New Hampshire, G106 Parsons Hall, Durham, NH 03824, USA

Accepted 30 September 2004
Available online 8 December 2004

Abstract

Determining the detailed morphology of composite latex particles in a confident manner is often very challenging and sometimes seemingly impossible. This paper reports on the details of an interlaboratory study, a so-called 'round robin' study, designed to determine the complete details of the particle structure of a particular styrene–acrylic copolymer latex system. Independent organizations received portions of the same composite latex and each performed several analytical measurements of the characteristics of the latex particles. Techniques included SEM, TEM, AFM, NMR, DSC, MFFT, GPC, CHDF and QELS. Each analytical test was performed by at least two independent laboratories using the protocols adopted by the individual organizations. Subsequently representatives from each of the six laboratories participated in a workshop to contribute their data, assess the results from all of the information developed, and to draw collective conclusions regarding the detailed structure of the particles. Complete morphology details must include the overall particle shape, the composition of its outermost region, and the internal structure. Multiple, complimentary sets of analytical data were necessary to confidently determine the particle structure, even for the well phase separated latex particles studied here.

Keywords: Latex; Morphology; Characterization

1. Introduction

Synthetic latex particles containing two or more individual polymers (called composite particles here) have found an extraordinary range of applications during the past 50-60 years. These include a wide variety of water borne coatings, impact modifiers for brittle plastics, pressure sensitive adhesives, and surface derivatized particles for medical diagnostics. Many people refer to these as 'core-shell' latices, although a review of the scientific and patent literature reveals that a rich tapestry of particle structures has been created-either measured or imagined. Indeed we know that in many cases it is not easy, or even possible, to create latices having particles with well defined core-shell structures. Due to the important applications of composite latex particles, there has been a significant amount of formulation–property studies undertaken to relate the final, mechanical properties to the chemistry and process techniques employed in their manufacture. However, there remains a large challenge in determining structure–property relationships, in other words, how the performance of these products depends upon the detailed structure of the composite particles. The challenge related to determining the specific details of the particle morphology is the subject of this communication.

Over the years a variety of analytical techniques have been used to measure the morphological characteristics of composite latex particles [1]. These techniques include microscopy, spectroscopy, thermal analysis, chromatography, and scattering techniques, among others. Electron microscopy has, in our opinion, made the single largest contribution. Although scanning electron microscopy (SEM) is sometimes a useful tool, the use of transmission electron microscopy (TEM) has had the greatest impact,

* Corresponding author. Tel.: +1 603 862 1878; fax: +1 603 862 4892.
E-mail address: don.sundberg@unh.edu (D.C. Sundberg).

0032-3861/$ - see front matter © 2004 Elsevier Ltd. All rights reserved.
doi:10.1016/j.polymer.2004.11.079

especially when the latex particles have been sectioned in a microtome prior to viewing in the TEM. Much more recently the use of atomic force microscopy (AFM) has added to the range of microscopic techniques, although AFM analysis is usually applied to whole latex particles, rather than sectioned ones. High energy neutrons or X-rays are scattered by the multiple polymer phases within composite particles and such scattering measurements have been made for a number of systems. However, the facilities required for using SANS or SAXS are not readily available to most investigators and thus such data are seldom available to many people. Solid-state nuclear magnetic resonance (NMR) has been used to characterize composite latex particles [2–4]. Despite the potential richness of the data that come from such experiments, not many investigators have taken advantage of it in comparison to the use of other techniques. On the other hand, thermal analysis techniques, particularly differential scanning calorimetry (DSC), are frequently used to characterize polymer blends [5–8] and are now being used more frequently with composite latex particles [9,10]. As will be discussed later in this paper, DSC and solid state NMR may offer complimentary data for analysis of internal particle structure. Lastly, those interested in coatings applications will use the minimum film formation temperature (MFFT) test to judge the narrow temperature range over which the dried latex transitions from a powder to an integral film.

Despite the advances in resolution and quality of data from the above analytical techniques, there remain substantial challenges to confidently relate such analytical data to particle structure. Part of this is associated with the 'art' required to prepare samples for analysis (e.g. recovering polymer from the latex and preparing it for TEM imaging without changing the inherent particle structure in the process) and in operating the instruments effectively. Another part is related to the utilization of raw data to obtain specific morphology information about the particle. Furthermore, all of the non-microscopic techniques mentioned above yield indirect, rather than direct, information about the particle structure.

Our experience has led us to conclude that a full specification of particle morphology requires one to assess (1) the overall shape of the composite particle, (2) the composition of the polymer present at the particle/water interface, and (3) the internal structure of the particle. More often than not, this specification requires data from more than one analytical technique. Yet the scientific literature, including some examples in our own papers, is replete with determinations of particle structure based upon TEM images alone. The reliance upon TEM images of only whole particles, rather than microtomed sections, makes the determination of particle structure particularly prone to artifacts and misinterpretation. This state of affairs motivated us to carry out an inter-laboratory study, a so-called 'round robin' study, to answer the following questions:

- What is the level of agreement between different laboratories for the data obtained from the same analytical technique at their individual locations?
- Do the data from different analytical techniques provide consistent information about the particle structure?
- What is the ability of a group of investigators from different labs to reach firm conclusions about particle morphology with the same data?

We approached this study by creating a latex produced at one location and then distributing the latex to all of the participants in the study for their own analyses. The goal was to have at least two labs develop independent data for each analytical technique. Then the participants met together to review all of the data and to strive to reach consensus on the full specification of particle morphology for the latex under consideration. The particular latex we used was anticipated to contain particles in which the individual polymers are well phase separated (and thus relatively simple in their structure) allowing us to clearly address all of the questions listed above. As such, this paper describes the details of developing and applying multiple sets of analytical data for a single latex system. In a subsequent paper we will focus on the morphology determination of increasingly complex latex systems in which phase separation within the particles is not so complete, thus posing challenges to the utility of some of the commonly used analytical techniques.

The participants of the study, in addition to ourselves (UNH), included researchers from Lund University, Sweden and from several industrial companies: Atofina, Surface Specialties UCB, NeoResins and Mitsubishi Chemicals.

2. Latex preparation and distribution

The chosen latex system was based upon a simple PMMA seed latex, with a second stage copolymer of P(styrene-*co*-butyl acrylate) having a T_g of 50 °C. The reaction temperature was 70 °C so that the seed polymer would be glassy and the second stage polymer would be soft during the polymerization. We prepared a 'pre-seed' latex of PMMA with a particle diameter of 71 nm (via CHDF) and at 5% solids content to form the basis for the seed latex process. Those particles were grown to the desired size by the batch-wise addition of MMA according to the recipe in Table 1. All reactions were carried out in a one litre, jacketed glass reactor at 70 °C under a nitrogen atmosphere with a paddle stirrer turning at 500 rpm. All chemicals were obtained from Acros Organics (New Jersey, USA). The water was deionized and previously boiled to remove dissolved oxygen, and the inhibitor was removed from the monomers by passing them through a column packed with alumina adsorption powder.

For the second stage polymerization, the comonomers

Table 1
Recipe for the seed latex polymerization

Pre-seed latex (g)	240.0
Water (g)	560.0
KPS[a] (g)	0.530
SDS[b], initial (g)	0.404
$NaHCO_3$ (g)	0.502
Monomer type	MMA
Monomer charge (g)	134.0
Monomer addition mode	Batch
Late SDS addition	
SDS (g)	0.601
Water (g)	19.5
Time of addition (min)	40
Reaction time (min)	150
Final solids content (wt%)	15.08

[a] Potassium persulfate.
[b] Sodium dodecyl sulfate.

were fed (using a Waters 501 HPLC pump) to the reactor so that a 'starve-fed' situation would be achieved, and samples were withdrawn to monitor the conversion rate (gravimetrically) to confirm the starve-fed nature. The recipe for this reaction is given in Table 2.

Small amounts of the composite latex were dried to powder form, and along with samples of the seed and composite latices themselves, were sent to all of the participating labs for analysis. The analyses were finished within 3 months of the preparation of the latex.

3. Characterization of the composite latex particles

In this section, the results from the various analytical techniques will be presented along with a description of the methods employed and the information provided by each technique. The interpretation of the results by the round robin group will be left for the discussion section.

3.1. Particle size measurements

Particle sizes were measured at UNH using capillary hydrodynamic fractionation (CHDF) with a Matec CHDF 2000, and at UCB Surface Specialties using dynamic light scattering (DLS) with a NICOMP particle analyzer from Particle Sizing Systems, Inc. The results are shown in Table 3 for the weight average (D_w) and number average (D_n) particle sizes and the polydispersity, $PD = D_w/D_n$.

Table 2
Recipe for the semi-batch second stage polymerization

Seed latex (g)	672.5
Water (g)	228.5
SDS (g)	0.458
$NaHCO_3$ (g)	0.153
Comonomer type and ratio (by weight)	30BA/70St
Comonomer charged (g)	82.0[a]
Comonomer feed rate (ml/min)	0.48[a]
Comonomer feed time (min)	184
Reaction time (min)	263
Final solids content (wt%)	18.53[a]

[a] The feed pump did not operate as planned and the actual feed rate and amount was 80% of design values.

The particle size measured by DLS at UCB Surface Specialties for the composite latex is somewhat larger that the corresponding value from CHDF at UNH. In all cases, the polydispersities are small and only one narrow peak was observed in the CHDF results, indicating a narrow particle size distribution and that secondary nucleation did not occur during the second stage polymerization. Comparative particle size studies for a single latex using multiple techniques have been reported [11,12] and generally show that DLS and CHDF yield similar results for monodispersed latex particles. Thus the reason for our discrepancy between DLS and CHDF results may be related to instrument calibration at that time, but we are unsure of this at the moment.

It is also useful to compare the seed particle size to the final size of the composite latex. Based on the stage ratio and the densities of the polymers, the expected volume ratio should be about 1.9. However, the actual volume ratio measured, from the weight average values at UNH, is 2.25. A possible reason for this apparent discrepancy will be discussed later.

3.2. Composition and molecular weight of the second stage copolymer

The molecular weight of the second stage polymer was measured at UNH using a Waters GPC with four styragel columns in series, three HMW 6E type and one HMW 7 type and equipped with both a refractive index detector (Waters 410) and a UV detector (Waters 486). The calibration was performed with polystyrene standards. It was possible to obtain the molecular weight of the second stage polymer (P(butyl acrylate-*co*-styrene)) directly by using the signal from the UV detector set at a wavelength of 254 nm, as the PMMA seed polymer does not absorb UV at this wavelength. The weight (M_w) and number (M_n) average molecular weights of the second stage polymer were found to be 1,352,000 and 300,280 g/mol, respectively.

^{13}C NMR was performed by Atofina, and determined that the second stage polymer was 69.9% styrene and 30.1% BA, by weight. This is close to the 73% styrene ratio used in the recipe. ^{13}C NMR was also used to determine the actual stage ratio of second stage polymer to seed polymer in the composite latex, and was determined to be 67%. This is significantly less than the 100% stage ratio as intended by the recipe, but is consistent with the fact that the Waters pump was found to be feeding monomer at only about 80% of the desired rate during the second stage polymerization. The additional discrepancy in the stage ratio is due to monomer losses from the reactor, mostly from the stirrer shaft inlet port, during the polymerization. These problems have been corrected but resulted in an effective stage ratio lower than that designed for this study. However

Table 3
Particle size measurements

	UNH results (CHDF)			UCB results (DLS)		
	D_w (nm)	D_n (nm)	PD	D_w (nm)	D_n (nm)	PD
Seed 1	162.7	159.6	1.019	–	–	–
Composite 1	213.3	211.2	1.01	241.2	235.8	1.03

disconcerting this may be, it does not change the subsequent morphology study.

3.3. Microscopy results

Scanning electron microscopy analysis was performed by Atofina and UNH. To prepare the sample, the latex was diluted drastically, dried on a glass slide and then coated with a thin metal film as is usual for SEM analysis of polymers. The images subsequently obtained are shown in Fig. 1(A) and (B).

Freeze-fracture SEM analysis was performed by NeoResins. The sample was prepared by dispersing the latex particles in a polymeric resin, freezing the sample, and then fracturing it. The fractured surface was then coated with a thin metal coating and observed in the SEM. The image obtained is shown in Fig. 2.

AFM analysis was performed by NeoResins, both in the tapping mode and in the contact mode. Contact mode AFM was also performed by UCB Surface Specialties. The results from tapping mode are shown in Fig. 3, and from contact mode in Fig. 4. It is clear from these figures that the tapping mode provides more detail and an image which is much easier to interpret, which is in agreement with the experience of other researchers [13]. Therefore, this appears to be the preferred mode of analysis for AFM of latex particles.

Transmission electron microscopy of the whole particle was performed at UNH by diluting the composite latex drastically and drying the diluted latex on a 300 mesh copper TEM grid that was coated with a nitrocellulose film to support the particles. This sample was then stained for approximately 10 min in RuO_4 vapor, and then observed in a JEOL 100S electron microscope at an accelerating voltage of 80 kV. A representative image obtained in this manner is shown in Fig. 5.

Transmission electron microscopy was also performed for microtomed sections of the latex particles at UNH, Lund University (Philips 120 BioTwin TEM) and Mitsubishi Chemical (JEOL JEM 2010 TEM, at an accelerating voltage

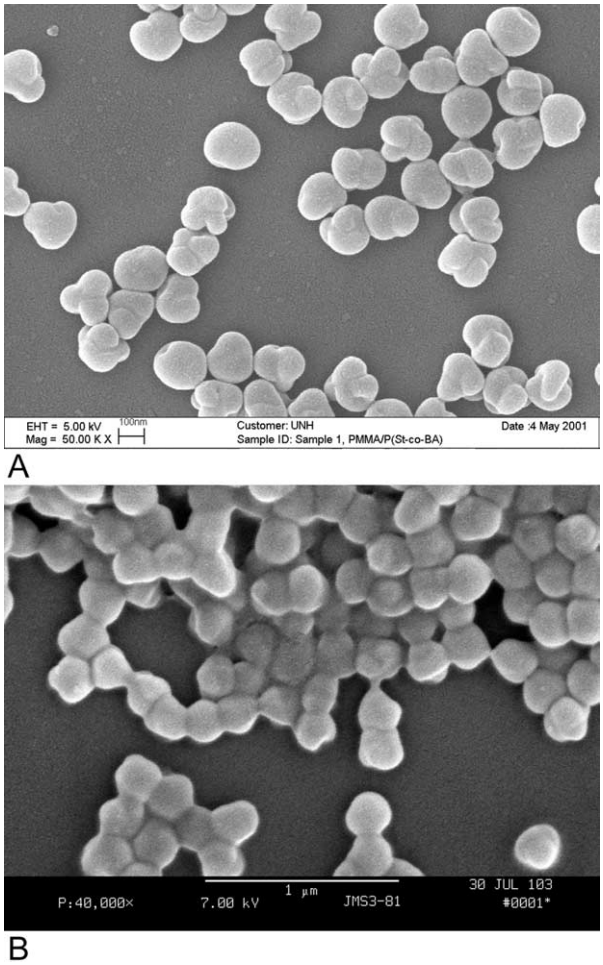

Fig. 1. SEM images obtained by (A) Atofina and (B) UNH.

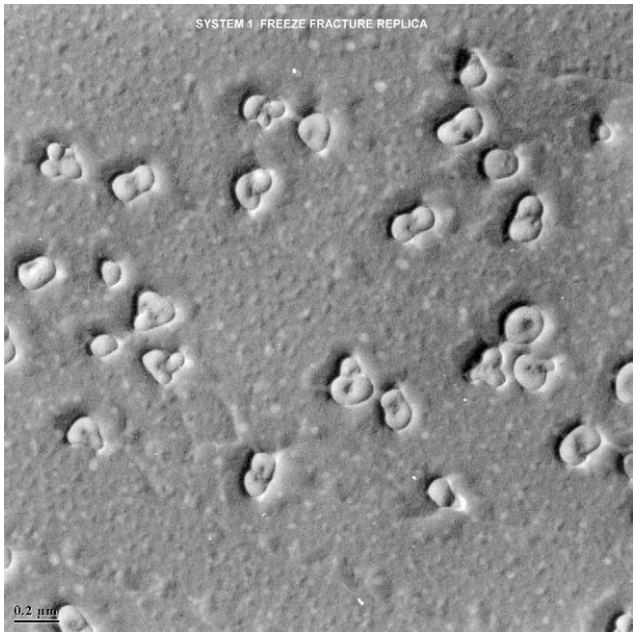

Fig. 2. Freeze fracture SEM image obtained by NeoResins.

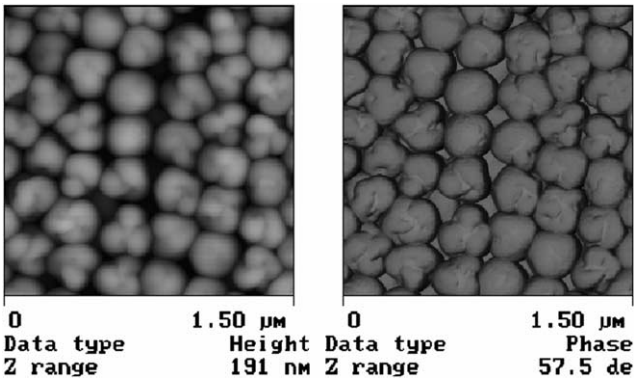

Fig. 3. Tapping mode AFM image obtained by NeoResins.

of 200 kV). Slightly different sample preparation methods and microscope settings were used in each case. In all cases the latex was dried at room temperature, which yielded a powder for this system because the T_g's of both polymers are significantly above room temperature. A small amount of this material was then embedded in an epoxy resin and sectioned using an ultracryomicrotome. The sections were then collected on copper TEM grids and in all cases they were stained in Ruthenium vapor. The differences in the sample preparation methods arise in the types of epoxy used.

The samples analyzed at Lund University used TAAB-812 epoxy that is commonly used for electron microscopy of polymers. However, the analysis at UNH used a simple two part epoxy (Z-Poxy™ manufactured by Pacer Technologies), because earlier experience had shown that EPON 812 (which is likely to be chemically similar to TAAB 812) epoxy monomers can plasticize the particles and drastically change their structure. It is clear from Fig. 6(A) that the particles are not plasticized by the Z-poxy (independent experiments have also confirmed this). Fig. 6(B) shows the image obtained by Mitsubishi. Unfortunately, it is not known which type of epoxy was used here, but it is clear

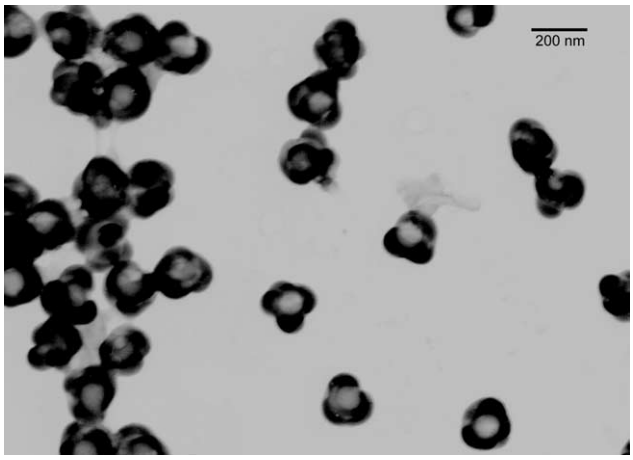

Fig. 5. Whole particle TEM image obtained by UNH, sample was stained for 10 min in RuO_4 vapor before imaging.

from the image that plasticization has not taken place. An alternate staining procedure was adopted by Lund to alleviate the plasticization problem. Fig. 6(C) shows a case where the dried sample was embedded directly in TAAB epoxy and then microtomed. The particles have clearly been plasticized because individual, separated particles, as observed in Fig. 6(A) and (B), are no longer apparent. Fig. 6(D) shows another result for which the dried sample was stained for 1 h in RuO_4 vapor before embedding in TAAB epoxy, followed by an additional 10 min of staining after microtoming. Clearly, RuO_4 staining prior to embedding prevents the particles from being plasticized, as the particles are separated and their structure is essentially the same as in Fig. 6(A) and (B). However, there are now small (10–20 nm in size) dark domains present, which are deposits of Ruthenium that condensed during the pre-embedding staining. They are only observed on the outside surfaces of the particles because the staining was done before microtoming.

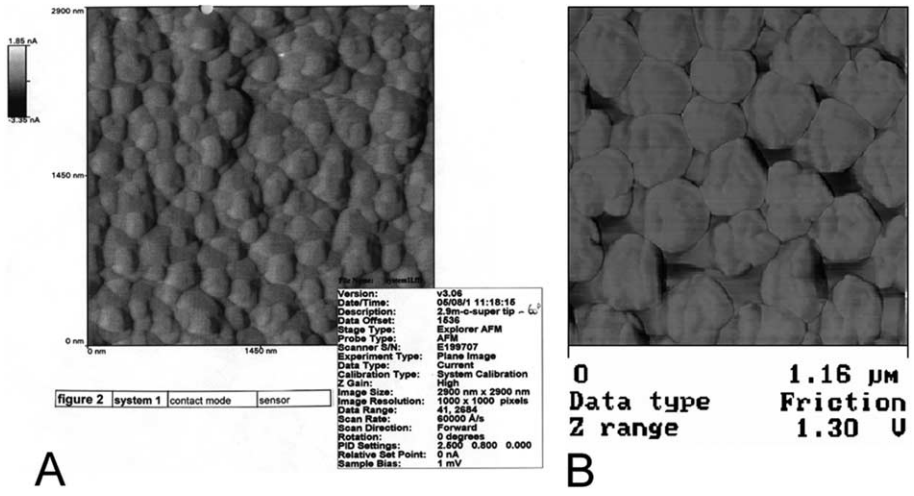

Fig. 4. Contact mode AFM images. (A) Obtained by Surface Specialties UCB, (B) obtained by NeoResins.

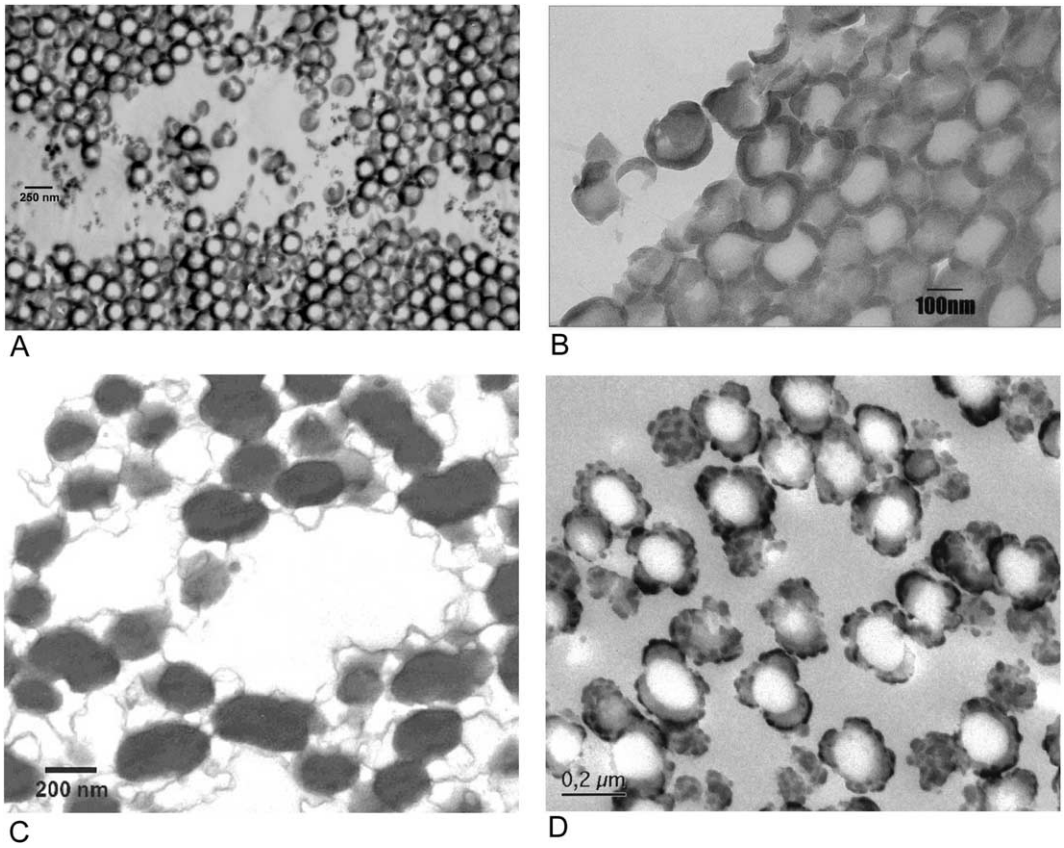

Fig. 6. Microtomed TEM images. All samples were stained with RuO_4 vapor after microtoming. (A) UNH, using Z-Poxy for embedding, (B) Mitsubishi, (C) Lund University, using TAAB 812 embedding resin without staining before embedding, (D) Lund University using TAAB 812 embedding resin, stained 1 h in RuO_4 vapor before embedding.

3.4. Differential scanning calorimetry results

In addition to detecting glass transitions and crystalline melting points in polymers, it has been shown that DSC can also be used to quantify the amount of interfacial material between the two polymer phases in polymer blends [5–8] and latex films [9,10]. This is done by comparing the magnitude of the ΔC_p's at the individual polymer glass transitions in a composite latex (or polymer blend) to the value of the ΔC_p for the corresponding pure polymer. Since two polymers are present in a composite latex, two distinct glass transitions are expected in the DSC trace. However, it is often observed that the magnitudes of ΔC_p at each transition are smaller than expected. The difference between the measured and expected values has been attributed to polymer that is present in interphase regions within the particles [5]. The amount of this interphase polymer can be quantified from the ΔC_p values.

DSC analysis was performed at both UNH and Surface Specialties UCB. The measurements at UNH were performed on a Perkin Elmer Pyris 1 DSC operating in the Step Scan mode, which is a technique similar to modulated DSC. Analysis at UCB was performed using a modulated temperature DSC from TA instruments. Results are shown in Fig. 7(A) and (B). In Fig. 7(A), the kinetic events have been removed by the Step Scan analysis, leaving only the thermodynamic transitions. In Fig. 7(B) the total heat flow, as well as the reversible and non reversible heat flow signals, are shown. The reversible heat flow signal (top curve in Fig. 7(B)) is relevant to the discussion here. Two distinct glass transitions are observed in both graphs in Fig. (7), as is expected for a well phase separated composite particle. The temperatures of the transitions are measured to be about 5° higher by Surface Specialties UCB than at UNH, which is most likely due to differences in the calibration of the two instruments and differences in the heating rate parameters. The T_g calculations from the analysis at UNH yielded ΔC_p values in addition to T_g's. The ΔC_p values, along with those for the pure seed and second stage polymers, are listed in Table 4 and used to calculate the percentage of each polymer in the interphase, which are also listed in Table 4. Following the lead of Hourston et al., the calculations utilized the following equation [7]:

$$\mathrm{Int_i} = \left(1 - \frac{\Delta C_p^i}{w_i \Delta C_p^{i0}}\right)$$

where $\mathrm{Int_i}$ is the percent of polymer i that is in the interphase, ΔC_p^i is the ΔC_p value measured for the composite at the transition corresponding to polymer i,

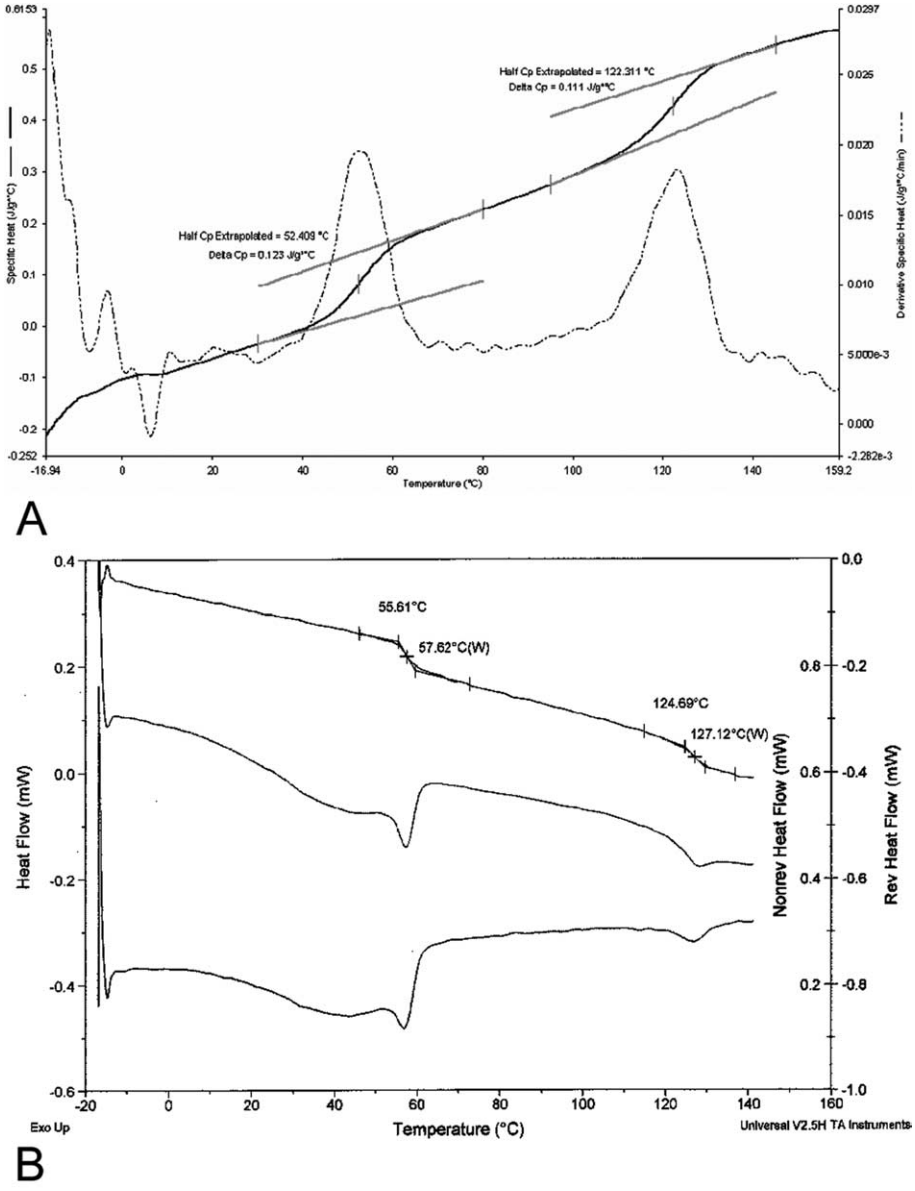

Fig. 7. DSC results for the composite samples. (A) UNH result using Step Scan DSC, (B) Surface Specialties UCB result using modulated DSC.

$\Delta C_p^{i,0}$ is the ΔC_p measured separately for pure polymer i and w_i is the weight fraction of polymer i in the composite.

For the DSC data presented here, we have always used the results obtained upon the first heating scan. Some researchers prefer the data from the second scan, however, as we will report in a later paper, we have found that it is important to consider the data from the first scan when trying to obtain information related to particle morphology. This is due to the fact that further phase separation of the polymers within the particles may occur upon thermal annealing in the DSC during the first heating scan (when above the T_g's of the two polymers) such that the information obtained upon the second scan may not be representative of the original state of the latex particles. In Fig. 7(A), the Step Scan DSC results are also plotted in derivative form so that the glass transitions appear as peaks, making it easier to visualize the extent of phase separation. The fact that two distinct T_g peaks are observed and that the curve returns essentially to baseline values in between the two peaks is evidence that the two polymers are highly phase separated and only a small amount of interphase material is present [5–10].

3.5. Solid state NMR results

Nuclear magnetic resonance in the solid state can provide important information regarding the internal composition of the various phases and interphases of composite particles [2–4]. If an interphase exists (a gradient of mobility), spin diffusion experiments can provide information about its structure and the total amount of material in the interphase regions, as well as the total amount of material in the

Table 4
Summarized results from DSC analysis.

	UNH results		Surf. Spec. UCB (T_g (°C))
	T_g (°C)	ΔC_p (J/g °C)	
Seed; PMMA	121.9	0.272	–
2nd Stage; P(BA-St)[a]	57.5	0.300	60.9
Composite seed transition	122.3	0.111	127.1
Composite 2nd stage transition	52.4	0.123	57.6
% seed in interphase	–	30%	–
% 2nd stage in interphase	–	4%	–

[a] The T_g and ΔC_p values for the second stage polymer was measured using a latex that were made separately and had the same ratio of styrene to butyl acrylate.

'mobile' and 'rigid' phases. The results do not provide information regarding the spatial location of the phases. Thus, in order to make more detailed conclusions about the particle morphology from this single technique, one must first make assumptions about the type of morphology that is present.

NMR spin diffusion analysis was performed by Atofina. The results indicated that only about 6% of the total material in the particles was present in an interphase region. Fig. 8 shows the amount of magnetization selected versus the strength of the dipolar filter for two different temperatures, 90 and 110 °C. The curve at 90 °C is perhaps more interesting, because this is half way between the T_g's of the pure seed and second stage polymers, so that the seed should be rigid and the second stage mobile at this temperature. This curve shows several 'steps', where the amount of mobile phase selected changes rapidly with changes in the dipolar filter strength. This type of behavior is an indication that the system does not possess an extended amount of interphase, which agrees qualitatively with the DSC results.

3.6. Film formation results

MFFT results were performed at NeoResins using a model SS-3000 MFFT instrument, manufactured by I.C.I. Ltd. The MFFT was taken to be the temperature at which a smooth, cohesive and transparent film is fully developed, and this was found to be at approximately 83 °C. This is intermediate between the T_g's of the seed and second stage polymers, and suggests that both polymers are influencing the film formation process.

3.7. Surfactant titration results

Surfactant titration of latex has been used for some time as a method of investigating latex particle morphology [14–18]. The principle is based on the fact that the adsorption area at maximum packing, A_s, for a given surfactant molecule is a function of the type of polymer forming the

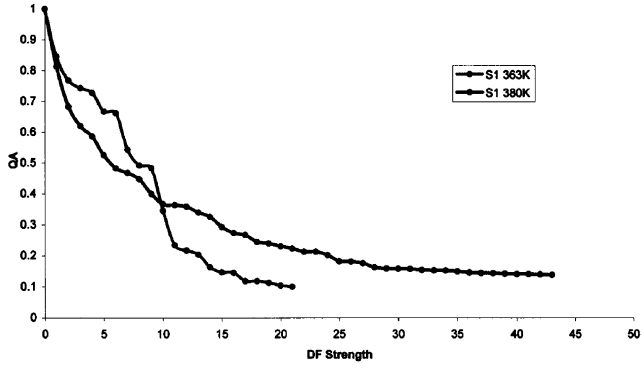

Fig. 8. Solid state NMR results from Atofina showing the amount of magnetization selected (QA) versus the strength of the dipolar filter (DF strength).

surface. More polar polymers absorb less surfactant than hydrophobic polymers. With knowledge of the A_s value for the pure seed and second stage polymers, the A_s value measured for the composite latex can be used to determine the percentage of the composite particle surface that is covered by either seed or second stage polymer. Surfactant titrations were performed at UNH and Surface Specialties UCB, using SDS as the titrating surfactant. Latices were first cleaned to remove surfactant and salts (residual initiator, buffer). The latices were cleaned at UNH by mixing the latex with a mixed bed of cationic and anionic resins (Barnstead-Thermolyne Corp.). At Surface Specialties UCB, they were cleaned by ultrafiltration. The cleaned latices were then titrated with a concentrated SDS solution (50 g/L) while monitoring the conductivity. The saturation point is observed as a change in slope of the conductivity vs. the amount of SDS added. The A_s values, along with the calculated % surface covered by the second stage polymer, are listed in Table 5. The results agree well between UNH and Surface Specialties UCB, although the Surface Specialties UCB A_s values are systematically slightly less than the UNH values, but the difference is within the range of the multiple titrations within a single lab. This is considered to be excellent agreement, especially in light of the fact that the two labs used entirely different methods to clean the latex samples.

4. Group assessment of the data sets

One of the most important elements of this study was that, after independently gathering data on the same latex using an array of different methods, the participants met as a group to discuss the results and collectively reach a conclusion about the morphology. As we began this process we concluded that we needed to structure our discussion, and decided to approach the process by striving to answer three major questions:

1. What is the overall shape of the particle?
2. Which polymer is covering the outermost surface of the particle, and if both then in what proportions?
3. What is the internal structure of the particle?

For each question we paid attention to a number of different issues. The first was to note which data sets could be used to answer that question. Next was whether or not there is consistency between the results from the same techniques but from different labs, and if there is agreement or contradiction between different techniques providing different but related information. Finally, is it necessary to have complimentary data sets in order to reach a detailed and confident conclusion?

4.1. Overall particle shape

Useful results came from AFM, SEM and the TEM of the whole particles. In Fig. 1 it is observed, somewhat surprisingly at first, that the particles are not spherical. Instead they have what appears to be a 'popcorn' type shape, having lobes protruding out from an otherwise spherical core. In addition, the projected area of the lobes on the surface is not circular, but they are clearly elongated and partially wrap around portions of the particle core. Based on our knowledge of the polymerization process, it is likely that the lobes would be second stage polymer, (P(BA-St)). However, it is not possible to make this distinction from the SEM image. The images from UNH and Atofina are in qualitative agreement with each other, as both reveal a non-spherical particle shape. However, the picture from Atofina shows a higher level of detail and allows more detailed conclusions about the lobed particle shape to be drawn.

AFM was conducted in both the tapping mode (Fig. 3) and contact mode (Fig. 4). Contact mode tests were performed by both NeoResins and Surface Specialties UCB, and the results are in qualitative agreement showing close packing of many particles and an apparent bumpy or irregular particle surface. However, the tapping mode results were far more detailed and revealing, and these were focused on by the group. The tapping mode AFM results are in perfect agreement with the SEM results with the overall particle shape revealed as being non-spherical and having lobes. Because the AFM was operated at room temperature, both the seed and second stage polymers were glassy and the AFM was not able to discern one polymer from the other. We did not attempt to use the AFM at a temperature between the T_g's of the two polymers where it

Table 5
Results from the SDS titrations

		Seed, PMMA[a]	2nd Stage, P(BA-St)[b]	Composite
Individual A_s (Å^2/molecule)	UNH	120	53.7; 50.7	79.3; 78.5, 77.5
	UCB	120	55; 58	78, 89
Average A_s (Å^2/molecule)	UNH	120	52.2	78.4
	UCB	120	56.5	83.5
% Surface that is 2nd stage polymer	UNH	–	–	41%
	UCB	–	–	37%

[a] The A_s for SDS on PMMA used was not measured directly for the seed latex, but is a value established from numerous previous measurements for PMMA at UNH.
[b] The A_s value on the second stage polymer was measured using a latex that was made separately, having the same ratio of styrene to butyl acrylate.

might have been possible to distinguish which polymer formed the lobes. Neither did we attempt to use chemically modified tips on the cantilever to try to distinguish between the polarities of polymers. We did briefly consider the possibility of using the force values obtained from the contact mode analysis as a judge of which type of polymer dominated the surface of the particles, thus offering information similar to that provided by surfactant titration. We found that the level of correlation between these force values and the polarity of the polymers for measurements on the pure seed and second stage polymers was poor, and therefore that we had little chance of using the method in this manner. However, we did not explore this deeply, and thus are unable to make conclusions on the potential of using AFM in such a manner.

Whole particle TEM was performed at UNH and shown in Fig. 5. This provides information about the shape of the particle because the particles are dried directly on a grid and not microtomed. The results obtained are different than the SEM and AFM due to the transmission nature of TEM, which removes the 3-dimensional nature of the images. However, it also makes it possible to obtain some amount of information about the internal structure in addition to the overall shape. In the TEM, the second stage P(BA-St) appears darker due to having a higher electron opacity and because it was selectively stained with RuO_4. In Fig. 5, the non-spherical, lobed structure of the particle is once again revealed, in agreement with the SEM and AFM results. However, we can now also determine that the lobes are in fact composed of P(BA-St) because they are much darker than the particle cores. Some of the particles reveal a light inner core of the PMMA seed, while others do not, depending on the orientation of the particle as it lies on the TEM grid.

The freeze fracture SEM results shown in Fig. 2 seem to require a certain level of experience to interpret them. This is related to trying to understand how the specimen fractured, and whether the particles themselves were fractured or simply 'pulled out' of the matrix when it was fractured. Unfortunately, no members of the group had extensive experience interpreting these types of experiments. The image does reveal a non-circular shape for the particles and in this sense is in agreement with the AFM, SEM and whole particle TEM results.

4.2. Outer surface of the particle

To answer this question, we found the results of the surfactant titration to be most useful. This comes from the fact that it is perhaps the only method that we used in this work that probes the composition of the outermost layer of the particles and can also provide quantitative information. Even if only a very thin layer of one polymer is present at the particle surface, it can be detected by surfactant titration. The microscopy methods, which may seem to provide information about the outer surface of the particles, would not in fact be able to detect a very thin layer. Also, when both polymers cover portions of the particle surface, microscopy is not able to easily quantify their fractional surface coverage. In concept it is possible that XPS or SIMS could also provide information about the very outer region of the particle, but neither were attempted in this study.

The results of SDS titrations in Table 5 show that about 40% of the particle surface is covered by the second stage P(BA-St), while the remaining 60% is composed of the seed polymer. As discussed previously, the agreement between titration's conducted at UNH and Surface Specialties UCB was excellent. This result fits well with the observation of a lobed morphology in the SEM and AFM results. It also agrees with the whole particle TEM result which shows that the lobes are composed of P(BA-St). While the whole particle TEM image also may suggest that the entire surface of the particles is not covered by these lobes, the surfactant titration's are able to confirm this and to quantify the extent of coverage by each polymer in a way that no other technique can. It should be noted that the values listed in Table 5 are subject to some amount of error, because our calculation of the total surface area of the latex particles assumed spherical particles, which is not true in this case. In addition, the lobed nature of the particle may affect the particle size measurements by CHDF and light scattering. Based on the overly large volume ratio calculated from the particle size measurements (presented earlier) compared to the known stage ratio, it is likely that the lobed structure leads to a false larger particle size being measured. Both factors (larger and spherical particle) would lead to smaller calculated values for A_s and a lower estimation of the percentage of second stage polymer on the surface. However, tests were performed in which the total particle surface area used in the calculations was varied and showed that these factors are not expected to alter the result to the point where it is not in agreement with a lobed morphology.

In addition to the surfactant titrations, the MFFT results also can provide some hints about which polymer covers the outer surface, although to a non-quantitative and more limited extent. The MFFT measured for this composite latex was about 83 °C. This is intermediate between the T_g's of the pure polymers and suggests that both polymers have some effect on the film formation process, which is in qualitative agreement with the fact that both polymers are present on the surface. However, based on the MFFT results alone one would not be able to make this conclusion, and would certainly not be able to quantify the fractional coverage by each polymer.

4.3. Internal structure of the particles

TEM of microtomed sections is perhaps the single most useful technique for gaining information about the internal structure. Whole particle TEM provides some information in this area, but features observed in the center of the particle image may actually be on the top or bottom of the

particle as it rests on the TEM grid. Microtomed TEM, because cross sections of particles are observed, can reveal the actual internal features of the particle and provides radial information about the internal particle structure.

The microtomed TEM photos obtained at UNH, Lund and Mitsubishi Chemical are presented in Fig. 6. The issue with the plasticization of particles by some epoxy was already discussed in the microscopy results section, so Fig. 6(C) is not relevant to the discussion here. Fig. 6(A), (B) and (D) all show that the core of the particle is light and roughly spherical and surrounded by darker material. This confirms that the core is composed of the PMMA seed polymer, while the outer regions are composed of the second stage P(BA-St). It is also clear that the particle cores are entirely free of domains of the second stage polymer, a result that could not be verified from the whole particle TEM. All three images are in general agreement, but differ in their degrees of clarity and detail and therefore in the amount of information provided. If the image in Fig. 6(A) is studied closely the lobed structure is somewhat apparent, but it would be difficult to notice if this was not known independently. The image in Fig. 6(B) shows the discontinuous nature of the particle shell more clearly, but it is not entirely apparent that there are separate lobes because many particles are packed together. The image in Fig. 6(D) clearly reveals the lobed structure, but also shows the dark ruthenium deposits on the outside of the particles.

TEM of microtomed sections, more than any other technique discussed thus far, has shown the possibility for significant lab to lab variation in the results and is very much dependent on the sample preparation and microscope operation techniques. There is also the largest possibility for having artifacts introduced during the sample preparation, such as particle plasticization by epoxy or over-staining by RuO_4, which if not properly understood could lead to false interpretations about the morphology.

DSC and solid state NMR also provide information about the internal structure of the particles because they can provide a measurement of the amount of interfacial material present, which is in turn dependent on the morphology. The DSC results presented in Table 4 suggest that about 30% of the seed polymer, and only about 4% of the second stage polymer, is present in an interphase (17% of the total). This shows that the polymers are well phase separated and the amount of interfacial material is low. This is also supported by the shape of the derivative Cp plot in Fig. 7(A). This result is consistent with the observed lobed morphology and with the fact that domains of P(BA-St) are not observed within the PMMA seed polymer cores, which would give rise to larger amounts of interphase.

From the NMR analysis conducted at Atofina, it was determined that about 6% of the total polymer was present in an interphase region, which is in rough agreement with the DSC result that there is very little interfacial material. The plot in Fig. 8 shows that when the measurement is performed at 90 °C, halfway between the T_g's of the two polymers, the amount of magnetization selected versus the dipolar filter strength shows a steep curve with a 'stepped' behavior. This is characteristic of well phase separated materials. When the measurement is performed at 110 °C the curve is more gradual and no longer stepped. This may be because the measurement temperature is approaching the T_g of the seed, and is well above that of the second stage polymer, so that both phases are now somewhat mobile.

4.4. Overall assessment of the morphology

The overall assessment agreed upon by the group is that the particle has a lobed type morphology with an inner core of PMMA that is roughly spherical and essentially free of internal occlusions of the second stage P(BA-St). This PMMA core is partially covered by lobes of the P(BA-St) which protrude out from the surface, giving the particle a non-spherical shape. The lobes are not circular in shape but rather are elongated along the surface. There is also very little mixing of the two polymers on the molecular scale, giving rise to very small amounts of interphase material. Fig. 9 provides a schematic representation of our collective morphology determination. This represents an ideal cross section of the particle, with the black phase being second stage polymer.

One of the most important messages of this study is that, in order to reach a detailed conclusion, it was necessary to have results from more than a single analytical technique. For each of the three questions, at least one technique was required that provided information related to that question. For instance, in order to determine the overall particle shape, AFM or SEM or whole particle TEM was required. AFM and SEM provided essentially the same information in this particular case, but slightly different information than whole particle TEM because of the 3-dimensional nature of the AFM and SEM images. However, whole particle TEM also provided some limited information about the internal structure and which polymer was in the lobes. The only technique that allowed us to determine conclusively which polymer was present on the outside surface of the particles and the extent to which it covered the surface was surfactant titration. In other systems, where one polymer might have a

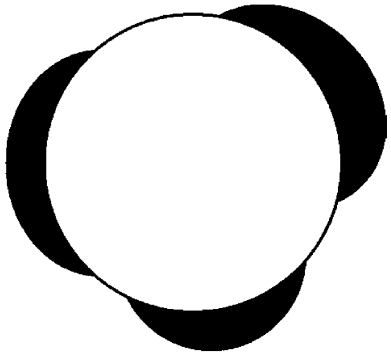

Fig. 9. Group assessment of the overall morphology.

T_g below room temperature and the other above, the AFM phase image may also have been able to provide information in this regard. Finally, microtomed TEM or DSC or NMR was needed to indicate that there were no internal domains within the particles. However, the microtomed TEM is preferred in this regard even though it is non-quantitative, as it provides a direct visual confirmation as well as spatial information. NMR and DSC provide quantitative information about interphase material that can be taken as an indication of whether or not small internal domains exist that would give rise to large amounts of interphase.

For this latex system, the combination of techniques having the minimum number and still leading to a firm conclusion are microtomed TEM, surfactant titration, and either SEM or AFM. In our collective opinion, if one of these techniques were removed, or replaced by another technique providing information about the same question, then the same conclusion may still have been reached but the level of confidence would have been diminished. If additional techniques are included above the minimum number, even if they provide less detailed information, this serves to strengthen any conclusion about the morphology by providing a cross check, which is normal good practice.

5. Further analysis through computer simulation

The composite latex was designed to have an inverted core-shell (ICS) morphology at thermodynamic equilibrium, but a non-equilibrium core-shell (CS) morphology was expected due to kinetic limitations. For this reason there was some surprise that the eventual particle structure featured lobes of the P(St-*co*-BA) copolymer on the surface of the PMMA seed particle. Why not a uniform coating of the P(St-*co*-BA) on the seed particle? In order to help us understand the potential reason for this reality, we turned to computer simulations of latex particle morphology. First, it is instructive to view the equilibrium morphology situation in terms of a surface free energy diagram for this composite latex particle. Fig. 10 shows the 3-dimensional free energy surface computed from a software package called UNHLATEX™_Eqmorph, the basics of which have been described in the literature [19]. The free energy of a CS structure is located at the top left hand corner of the energy surface. This energy surface shows that an ICS morphology is strongly favored as the equilibrium structure because it has the lowest free energy, corresponding to the lower right hand point.

Second, the realities of the actual polymerization conditions (reaction temperature $<T_g$ of the seed polymer and a starve fed polymerization) dictated that the second stage polymer radicals would not likely penetrate the seed latex particle to any significant extent during the reaction. Modeling of this situation was performed with a software package called UNHLATEX™_Kmorph that has been described in significant detail in the literature [20,21].

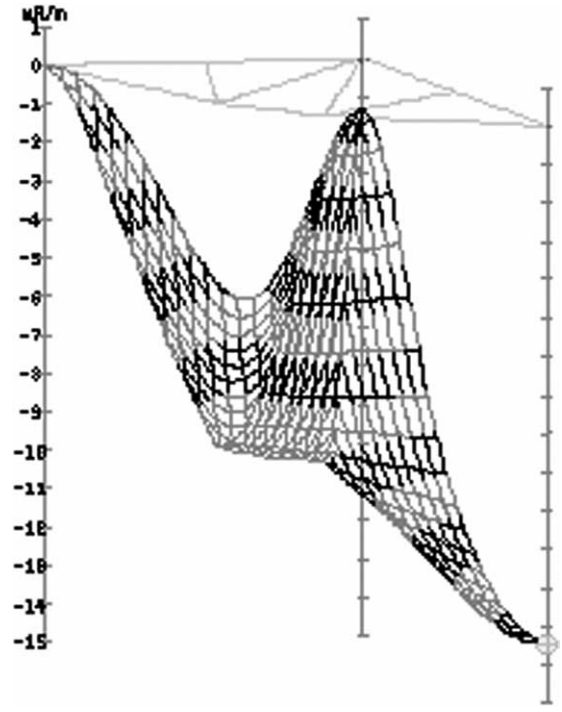

Fig. 10. Prediction of the equilibrium morphology from simulations performed with the UNHLATEX™_Eqmorph software.

These calculations use the diffusion coefficients of the growing oligomeric radical chains to predict the extent to which the second stage polymers penetrate the seed polymer particle. The result is shown in Fig. 11, which represents an ideal microtomed section of the particle as it would appear in the TEM with appropriate contrast between the two phases. Clearly the predictions favor the St/BA copolymer

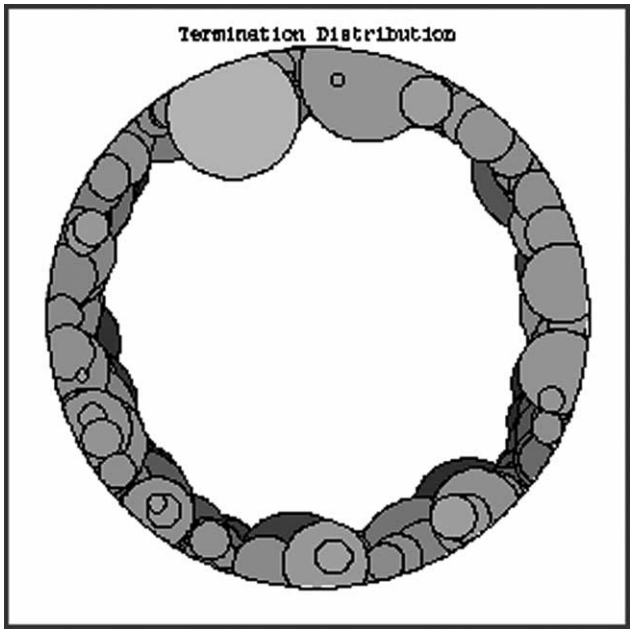

Fig. 11. Prediction of the kinetically controlled morphology from simulations performed with the UNHLATEX™_Kmorph software.

to be on the outside of the particle, and this core-shell arrangement is what we had imagined when we made the latex. However, the large energy difference between the CS and ICS morphologies predicted in Fig. 10 shows a large driving force for forming an ICS structure rather than a CS.

To assist us in understanding the reasons for the observed lobed morphology we used another feature of the Eqmorph software which computes the relative free energy of several different non-equilibrium structures. As seen in Fig. 12, a number of possible structures are considered where the light phase is the second stage polymer and the dark phase is the seed polymer.

The equilibrium free energy (Gibbs free energy per unit surface area of the seed latex particle) is shown as the dotted line at the bottom of the diagram, at −13.47 mN/m. The free energy of the corresponding core-shell arrangement is zero (the reference point from which all other free energies are computed). The solid bars show the free energy decrease for other possible structures compared to the core-shell structure. The distance between the dotted line and the bottom of the bar shows the free energy increase compared to the equilibrium morphology. With that, we ask the reader to look at the fifth structure from the left, which shows a 'sandwich' structure having two partial hemispheres partially surrounding the seed polymer. This can be roughly viewed as a seed particle (misshapen) with two, equal sized lobes of second stage polymer on its surface, and is therefore most similar to the observed morphology in the present system. This structure has a free energy about midway between those of the CS and the ICS morphologies. This strikes a balance between having the water phase exposed to purely polar or non-polar polymer phases, with a consistent internal polymer/polymer interface. Thus, a lobed structure has substantially less surface free energy than the core-shell and is the preferred morphology if the choice were only between those two possibilities. In the present case, since it was impossible for the particle to achieve its true equilibrium ICS structure due to kinetic limitations, it appears to have arranged itself into the lowest free energy state of the remaining alternatives. Thus it must be that the St/BA copolymer with its T_g of about 50 °C, being soft at the reaction temperature of 70 °C, was able to move along the surface of the PMMA particle to assemble itself into lobes that provided a lower relative energy state than the full surface coverage characteristic of a CS arrangement.

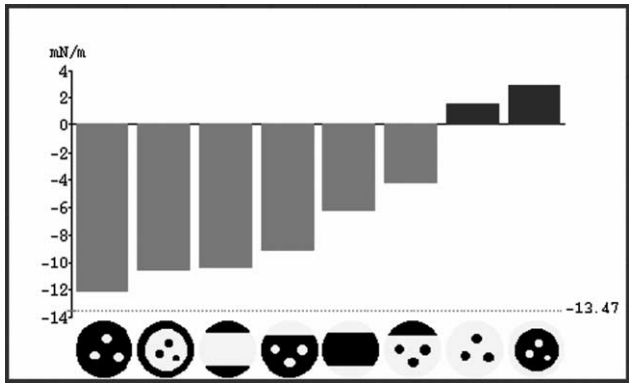

Fig. 12. Comparisons of the surface free energies of various non-equilibrium morphologies from simulations performed with the UNHLA-TEX™_Eqmorph software.

6. Conclusions

Working through this type of round robin study has led us to the conclusion that a complete morphology determination requires characterization of three major aspects of the particle structure, these being (1) the overall particle shape, (2) the composition of the surface of the particle and (3) the internal structure of the particle. It is necessary to employ a range of complimentary analytical techniques because one single technique will seldom, if ever, provide information about all three of these aspects, even for simple systems. The results of various methods must show consistency and cannot contradict one another, and having multiple perspectives provided by a number of techniques serves to increase the level of confidence and detail in the final morphology determination.

For the system studied here, we are completely confident of the conclusion reached by the group because all of the above requirements were met. The agreement between different labs for the same analytical technique was in general very good, especially for the non-microscopy techniques such as DSC and surfactant titration. However, the microscopy techniques, especially TEM, while being in general agreement also showed the most variation between labs. This is a direct result of the sample preparation methods employed and the fact that these techniques require a high level of operator skill, which can affect the quality of the results obtained. The importance of this observation is highlighted by the fact that TEM methods are perhaps the most commonly applied of all the various techniques for morphology determination, and because most investigators tend to fall back on a method that provides a visual representation of the particle morphology. Of course, the system studied here was simple and straightforward compared to many experimental and industrial latices. The difficulties encountered as a result of changing the characteristics of the latex system towards increasing complexity will be addressed in future papers.

Acknowledgements

We would like to thank the participating companies, universities and the individual researchers for making this work possible: John Verstegen from UCB Surface Specialties, Kiichi Itoh from Mitsubishi Chemical; Richard Brown and Tijs Nabuurs from NeoResins, Claude Granel and

Michel Valtier from Atofina, and Ola Karlsson and Helen Hassander from Lund University, Sweden.

References

[1] Durant YG, Sundberg DC. Polym React Eng 2003;11(3):433–55 and references therein.
[2] Landfester K, Spiess HW. Acta Polymerica 1998;49:451–64.
[3] Kirsch S, Landfester K, Schaffer O, El-Aasser MS. Acta Polymerica 1999;50:347–62.
[4] Tsavalas JG, Schork FJ, Landfester K. JCT Res 2004;1(1):53–63.
[5] Hourston DJ, Song M. J Appl Polym Sci 2000;76:1791–8.
[6] Song M, Hammiche A, Pollock HM, Hourston DJ, Reading M. Polymer 1995;36(17):3313–6.
[7] Hourston DJ, Song M, Hammiche A, Pollock HM, Reading M. Polymer 1997;38(1):1–7.
[8] Swier S, Van Mele B. Polymer 2003;44:6789–806.
[9] Hourston DJ, Song M, Pang Y. J Brazilian Chem Soc 2001;12(1):87–92.
[10] Hourston DJ, Zhang HX, Song M, Pollock HM, Hammiche A. Thermochimica Acta 1997;294:23–31.
[11] Elizalde O, Leal GP, Leiza JR. Particle Particle Syst Character 2001;17(5–6):236–43.
[12] Schneider M, McKenna TF. Particle Particle Syst Character 2002;19(1):28–37.
[13] Sommer F, Duc TM, Pirri R, Meunier G, Quet C. Langmuir 1995;11:440–8.
[14] Paxton TR. J Colloid Interface Sci 1969;31(1):19–29.
[15] Vijayendran BR. J Appl Polym Sci 1979;23:733–42.
[16] Okubo M, Yamada A, Matsumoto T. J Polym Sci: Polym Chem Ed 1980;16:3219–28.
[17] Piirma I, Chen SR. J Colloid Interface Sci 1980;74(1):90–102.
[18] Stubbs JM, Durant YG, Sundberg DC. Langmuir 1999;15(9):3250–5.
[19] Durant YG, Sundberg DC. J Appl Polym Sci 1995;58(9):1607–18.
[20] Karlsson OJ, Stubbs JM, Carrier RH, Sundberg DC. Polym React Eng 2003;11(4):589–625.
[21] Stubbs JM, Carrier RC, Karlsson OJ, Sundberg DC. Prog Colloid Polym Sci 2003;124:131–7.